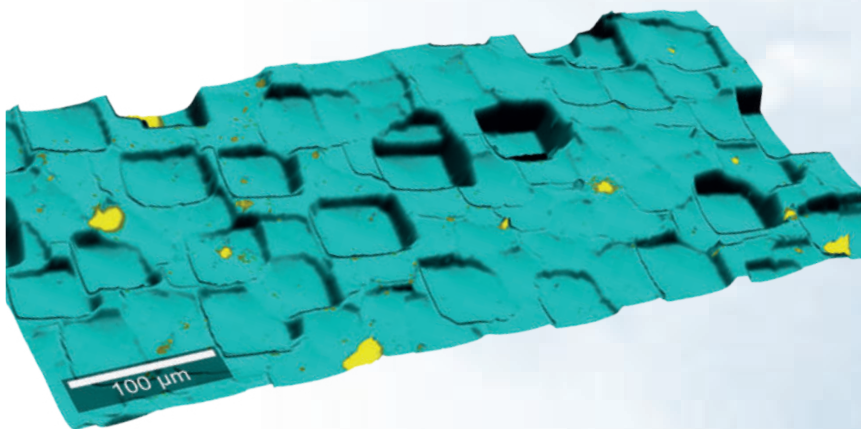
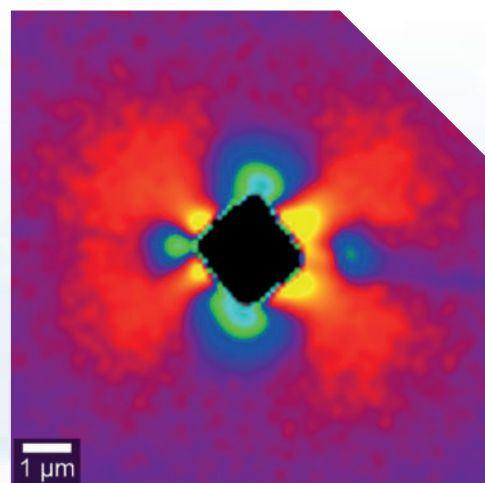
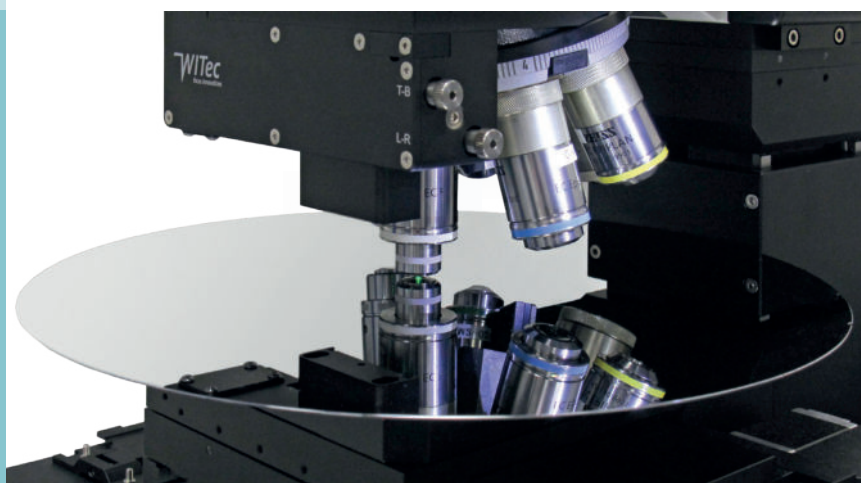


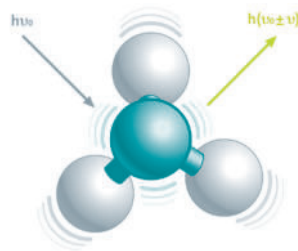
# Correlative Raman Imaging of Semiconducting Materials



Confocal Raman microscopy is a non-destructive analysis method that is uniquely capable of characterizing semiconducting materials. It can reveal the chemical composition of a sample, identify possible contaminants and even visualize strain fields in 3D volumes. In combination with techniques such as AFM or SEM, semiconducting materials can be investigated more comprehensively.

## The Raman principle

The Raman effect is based on the inelastic scattering of light by the molecules of gaseous, liquid or solid materials. The interaction of a molecule with photons causes vibrations of its chemical bonds, leading to specific energy shifts in the scattered light. Thus, any given chemical compound produces a particular Raman spectrum when excited and can be easily identified by this individual “fingerprint.” Raman spectroscopy is a well-established, label-free and non-destructive method for analyzing the molecular composition of a sample.



## Raman imaging

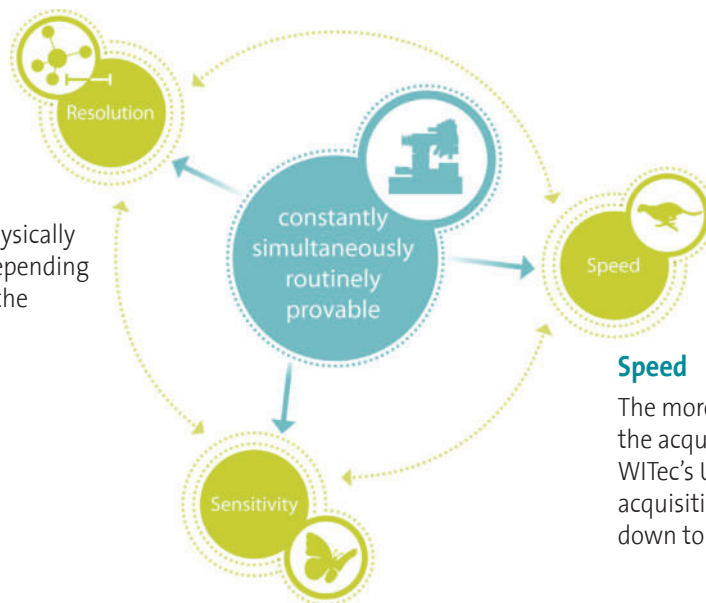
In Raman imaging, a confocal microscope is combined with a spectrometer and a Raman spectrum is recorded at every image pixel. The resulting Raman image visualizes the distribution of the sample’s compounds. Due to the high confocality of WITec Raman systems, volume scans and 3D images can also be generated.

## No need for compromises

The Raman effect is extremely weak, so every Raman photon is important for imaging. Therefore WITec Raman imaging systems combine an exceptionally sensitive confocal microscope with an ultra-high throughput spectrometer (UHTS). Precise adjustment of all optical and mechanical elements guarantees the highest resolution, outstanding speed and extraordinary sensitivity - simultaneously! This optimization allows the detection of Raman signals of even weak Raman scatterers and extremely low material concentrations or volumes with the lowest excitation energy levels. This is an unrivaled advantage of WITec systems.

### Resolution

Lateral resolution is physically limited to ~200 nm, depending on the wavelength of the incident light.



### Speed

The more sensitive a system is, the shorter the acquisition time for a single spectrum. WITec’s Ultrafast Raman Imaging reduces acquisition times for single Raman spectra down to well below 1 ms.

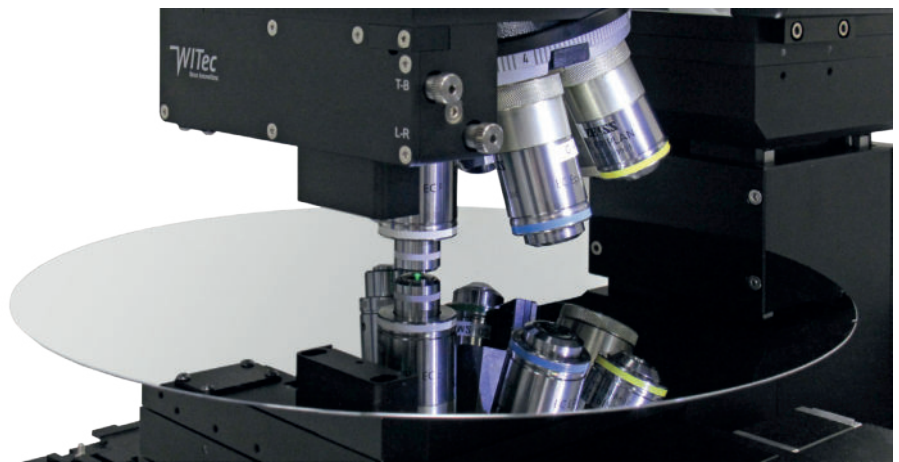
### Sensitivity

A high confocality increases the signal-to-noise ratio by reducing the background. With the UHTS Series, WITec developed lens-based, wavelength-optimized spectrometers with a spectral resolution down to 0.1 cm<sup>-1</sup> relative wavenumbers.

## Correlative Raman Imaging of Semiconducting Materials

Semiconducting materials are the basis for many electronic and optoelectronic devices such as light-emitting diodes (LED), laser diodes, photodiodes, solar cells and integrated circuits. Prominent examples of semiconducting materials include silicon (Si), silicon carbide (SiC), gallium arsenide (GaAs) and gallium nitride (GaN). In addition, 2D materials, such as molybdenum disulfide (MoS<sub>2</sub>), are the focus of extensive research due to their potential in the field of semiconductors. During research, fabrication and quality control, the structure of the crystals as well as defects and stress fields in the crystals must be detected efficiently and without damaging the sample in order to produce high-quality devices. Raman microscopy is ideally suited to this task.

This application note presents several examples of studies on semiconducting materials using 2D and 3D Raman imaging in combination with various other techniques such as atomic force microscopy (AFM), scanning electron microscopy (SEM) or second harmonic generation (SHG) microscopy. Raman imaging can distinguish between the semiconducting material and possible contaminants and identify them chemically. It can reveal stress fields in the crystal, even in 3D in some samples. At the same time, AFM and SEM yield information on the sample's topography. Thus, the combination of these techniques enables detailed sample characterization.



*Silicon wafer inspection with a WITec alpha300 confocal Raman microscope*

## Correlative topography and Raman measurements

When investigating semiconducting materials, the sample's surface structure is often of interest. WITec TrueSurface technology obtains topographic and chemical information simultaneously by combining a Raman microscope with an optical profilometer. Additionally, the profilometry data is used for focus stabilization, so that even rough, irregularly-shaped and inclined surfaces are kept in focus during the Raman measurement [1]. The application example in Figure 1 shows the topographic Raman image of multi-crystalline silicon. The height difference between the areas was up to 9 μm and the measurements were performed with a 100x objective featuring a depth resolution of about 900 nm. Nevertheless, the surface was kept in focus by TrueSurface over the entire measured region.

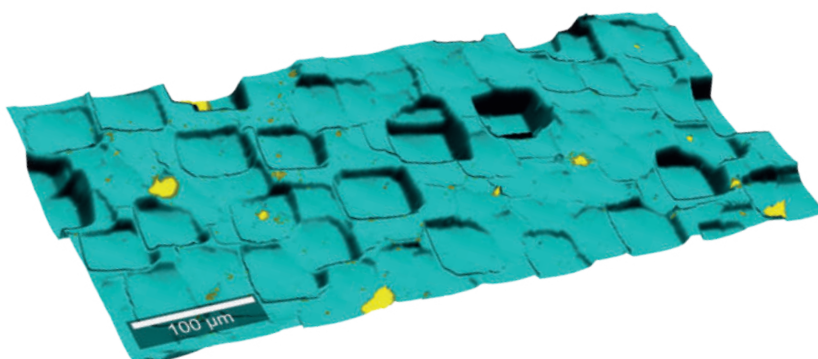


**Figure 1: Topography and chemical composition of multi-crystalline silicon.** The surface structure information and Raman image were recorded simultaneously using TrueSurface technology and overlaid. The Raman signal from silicon is color coded in turquoise and the yellow spots represent areas of increased fluorescence signal.

## 3D Raman imaging of stress fields

Gallium nitride (GaN) is a direct band gap semiconductor commonly used, for example, in light-emitting diodes, solar cells and transistors. In order to obtain high-quality GaN crystals with a low density of dislocations, the material can be grown on structured substrates. To evaluate the growth methods and the produced materials, non-destructive techniques are needed for detecting stress in the crystals.

In the example presented here, a 20  $\mu\text{m}$ -thick layer of GaN was grown on a patterned sapphire substrate in a two-step process, using metal organic vapor phase epitaxy and hydride vapor phase epitaxy. The substrate featured evenly-spaced hexagonal pits. The sample was provided

courtesy of Dr. Eberhard Richter from the Materials Technology Department of the Ferdinand Braun Institute, Berlin, Germany, where fabrication of the pattern and GaN growth were performed. Stress fields in the crystal were then investigated by 3D confocal Raman imaging using a WITec alpha300 Raman microscope equipped with an ultra-high throughput spectrometer (UHTS).

First, an overview white-light image was acquired using a 100x air objective with NA 0.9 (Figure 2). As GaN is transparent for visible light, the honeycomb-like structure of the substrate is visible beneath the GaN layer. The sample was then investigated in detail by 3D Raman imaging using an excitation wavelength of 532 nm.

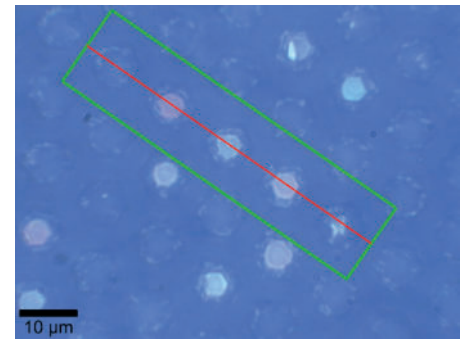


**Figure 2: White-light image of a GaN crystal grown on a patterned sapphire substrate.** The hexagonal structure of the substrate is visible through the 20  $\mu\text{m}$ -thick GaN layer grown on top. A Raman depth scan was performed along the red line and a z-stack of 20 x-y scans was recorded in the green area (see Figure 3).

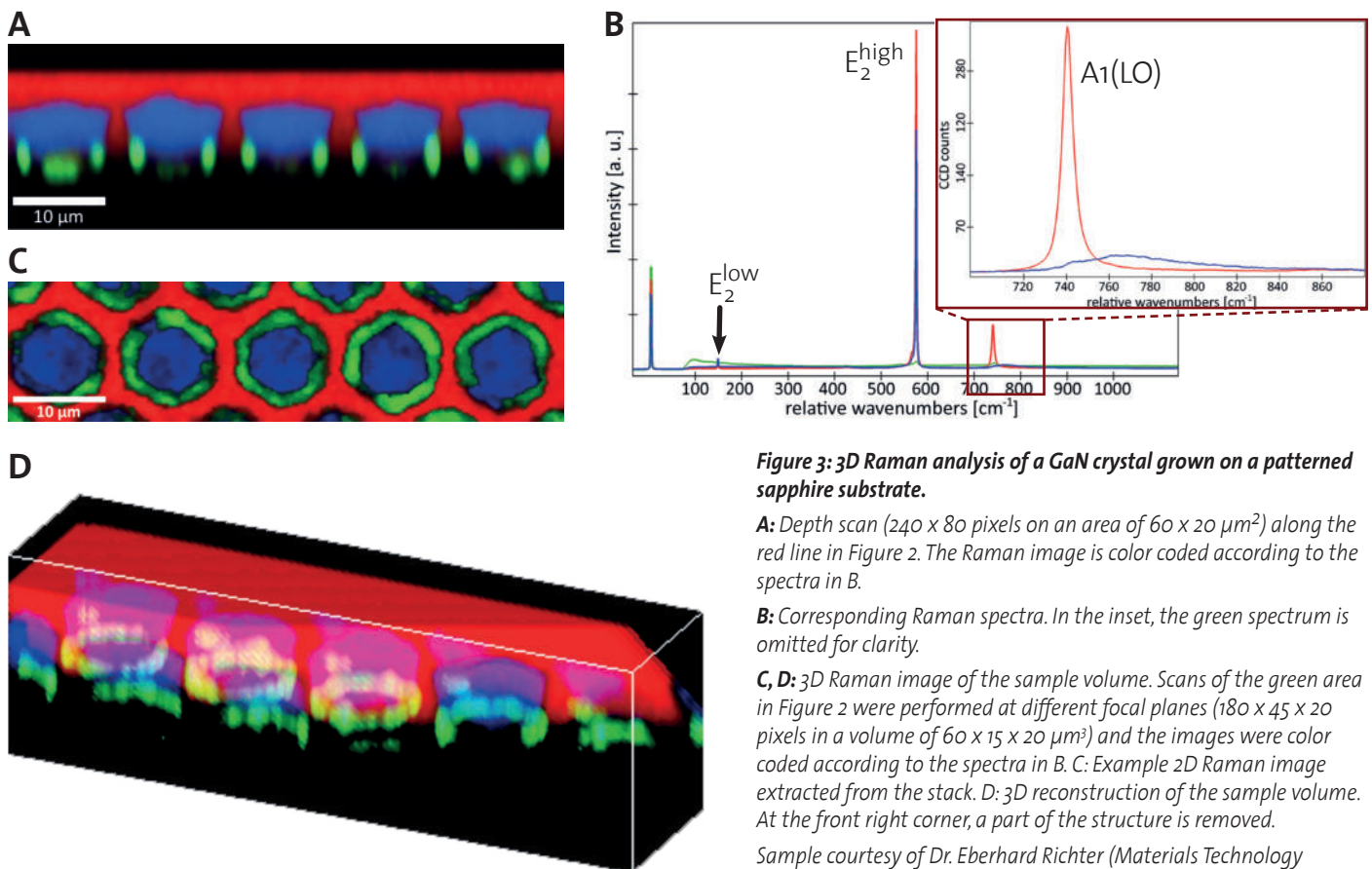


**Figure 3: 3D Raman analysis of a GaN crystal grown on a patterned sapphire substrate.**

**A:** Depth scan (240 x 80 pixels on an area of 60 x 20  $\mu\text{m}^2$ ) along the red line in Figure 2. The Raman image is color coded according to the spectra in B.

**B:** Corresponding Raman spectra. In the inset, the green spectrum is omitted for clarity.

**C, D:** 3D Raman image of the sample volume. Scans of the green area in Figure 2 were performed at different focal planes (180 x 45 x 20 pixels in a volume of 60 x 15 x 20  $\mu\text{m}^3$ ) and the images were color coded according to the spectra in B. C: Example 2D Raman image extracted from the stack. D: 3D reconstruction of the sample volume. At the front right corner, a part of the structure is removed.

Sample courtesy of Dr. Eberhard Richter (Materials Technology Department of the Ferdinand Braun Institute, Berlin, Germany).

A 2D depth scan was performed along the red line in Figure 2 and a Raman spectrum was recorded at each pixel. The resulting Raman image (Figure 3A) was color coded according to the measured spectra (Figure 3B), revealing three distinct areas in the sample. The red spectrum shows the typical features of GaN [2] and is dominant at the surface of the GaN layer, showing that the crystal grown there was high in quality. The green spectrum shows enhanced fluorescence at low wavenumbers and is found only at the walls of the pits in the substrate. Most likely, it is a remnant of the etching process. The blue spectrum measured above the pits is distinct from the red one, mainly at the  $A_1(\text{LO})$  peak near  $740\text{ cm}^{-1}$  (Figure 3B, inset). This peak is upshifted and strongly broadened compared to the red spectrum, indicating a lower quality GaN crystal in the areas above the pits (blue) compared to the regions at the surface (red). Next, a stack of 2D scans was performed at different focal planes of the area indicated

in Figure 2. Figure 3C shows one layer from the stack, in which the discussed spectral features are again visible. A 3D representation of the sample volume was generated from the image stack (Figure 3D). The fluorescence signal (green) forms a ring at the walls of the pits, while the space on top of the pits is dominated by the distorted GaN spectrum (blue). The topmost layers are characterized by the undistorted GaN spectrum (red).

Strain in crystalline samples is often associated with Raman peak shifts. In order to reveal stress fields in the GaN sample, a peak shift analysis was performed for the entire z-stack. The position of the  $E_2^{\text{high}}$  peak near  $570\text{ cm}^{-1}$  was quantified for each spectrum by fitting a Lorentzian function. Figure 4 shows a 3D reconstruction of the same sample volume as in Figure 3D, but color coded according to the determined peak shift. The positions of the pits in the substrate are indicated by the picture in the bottom plane. The stress fields propagate from the interface to the surface

mainly in tube-like structures, which become narrower towards the surface, again indicating that the GaN crystal quality is higher at the surface than close to the interface. However, the overall differences in the peak positions were quite small ( $< 1\text{ cm}^{-1}$ ) and thus, the overall differences in the strain of the GaN crystal were also small. Nevertheless, the peak shift sensitivity of the UHTS300 spectrometer was sufficient to measure and visualize them.

Using a similar approach, Joonas Holmi (Aalto University, Finland) and co-workers recently published a method for characterizing threading dislocations (TDs) in ammonothermally-grown  $\alpha$ -GaN crystals using 3D Raman microscopy [3]. By quantifying the Raman peak shift of the  $E_2^{\text{H}}$  peak at each position, they were able to locate the distortions, estimate the TD density in their sample and visualize the propagation of the stress fields into the crystal volume in 3D. Their measurements even enabled them to distinguish between edge  $\vec{a}$ -type and mixed  $\vec{a}+\vec{c}$ -type TDs [3].

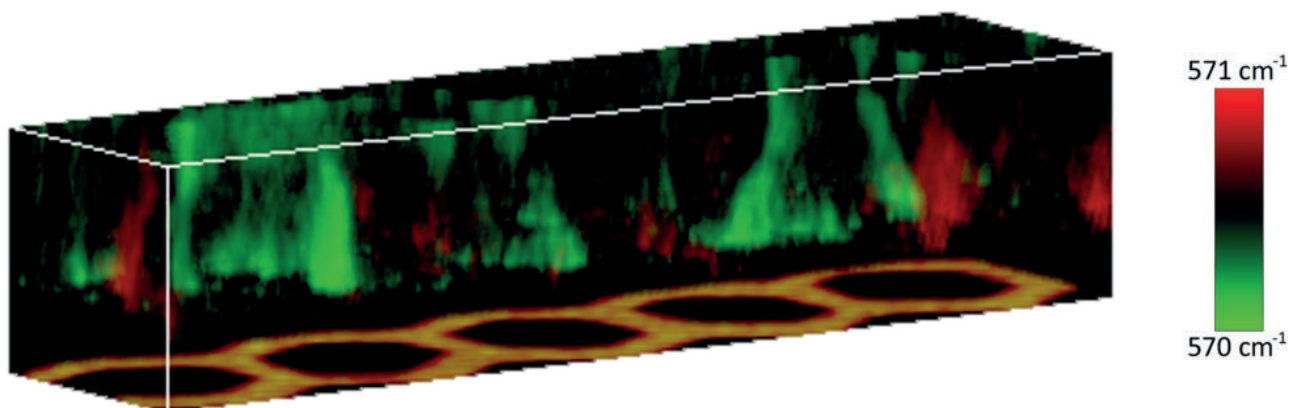


**Figure 4:** 3D representation of stress fields in the GaN crystal (the same sample volume as in Figure 3D). The position of the  $E_2^{\text{high}}$  Raman peak near  $570\text{ cm}^{-1}$  is color coded, revealing stress fields in the crystal. The image in the bottom plane indicates the positions of the pits. Sample courtesy of Dr. Eberhard Richter (Materials Technology Department of the Ferdinand Braun Institute, Berlin, Germany).

## Stress in silicon – correlative Raman-AFM imaging

When characterizing materials, the effect that deforming forces have on them is often of interest. In a Vickers test, a square-based diamond pyramid is pushed into the sample material with a controlled force. From the size of the resulting indent, a value for the material's hardness can be obtained. Such microindents can be efficiently characterized using a combination of atomic force microscopy (AFM) and Raman imaging [4]. In this example, the indentation was made with a force of 50 mN in a silicon (111) substrate using a Fischer Indentation System. Raman and AFM images were acquired at precisely the same sample position using an alpha300 RA combined Raman-AFM microscope.

Indentation resulted in a pyramidal indent of 2.6  $\mu\text{m}$  diagonal length with protrusions at the edges (Figure 5A). The indent was 160 nm deep and the protrusions were about 7 nm high (Figure 5B). The observed deformations caused stress in the silicon around the indent, which was visualized by Raman imaging. For every recorded Raman spectrum, the relative shift of the silicon peak at  $520\text{ cm}^{-1}$  was quantified and color coded in the Raman image (Figure 5C). As stress leads to peak shifts in the Raman spectra, the symmetric stress fields around the indent are visible in this image [4, 5]. Tensile strain occurred at the corners of the pyramidal indent (shift to lower wavenumbers, blue/green areas in Figure 5C) and compressive strain

at the protruding sides (shift to higher wavenumbers, yellow/red areas in Figure 5C). Stress profiles along three different axes of the indent are displayed in Figure 5D. In a statistical analysis of the stress-free areas, the standard deviation of the Raman peak position was about  $0.02\text{ cm}^{-1}$  (see also Cross Section 1 in Figure 5D). In silicon, a peak shift of  $1\text{ cm}^{-1}$  corresponds to a stress of 435 MPa [4]. Thus, the precision of  $0.02\text{ cm}^{-1}$  corresponds to a stress sensitivity of less than 9 MPa. This high degree of precision was achieved with an integration time of 70 ms per spectrum. The example illustrates the usefulness of correlative Raman-AFM measurements for characterizing topography and strain in semiconducting materials.

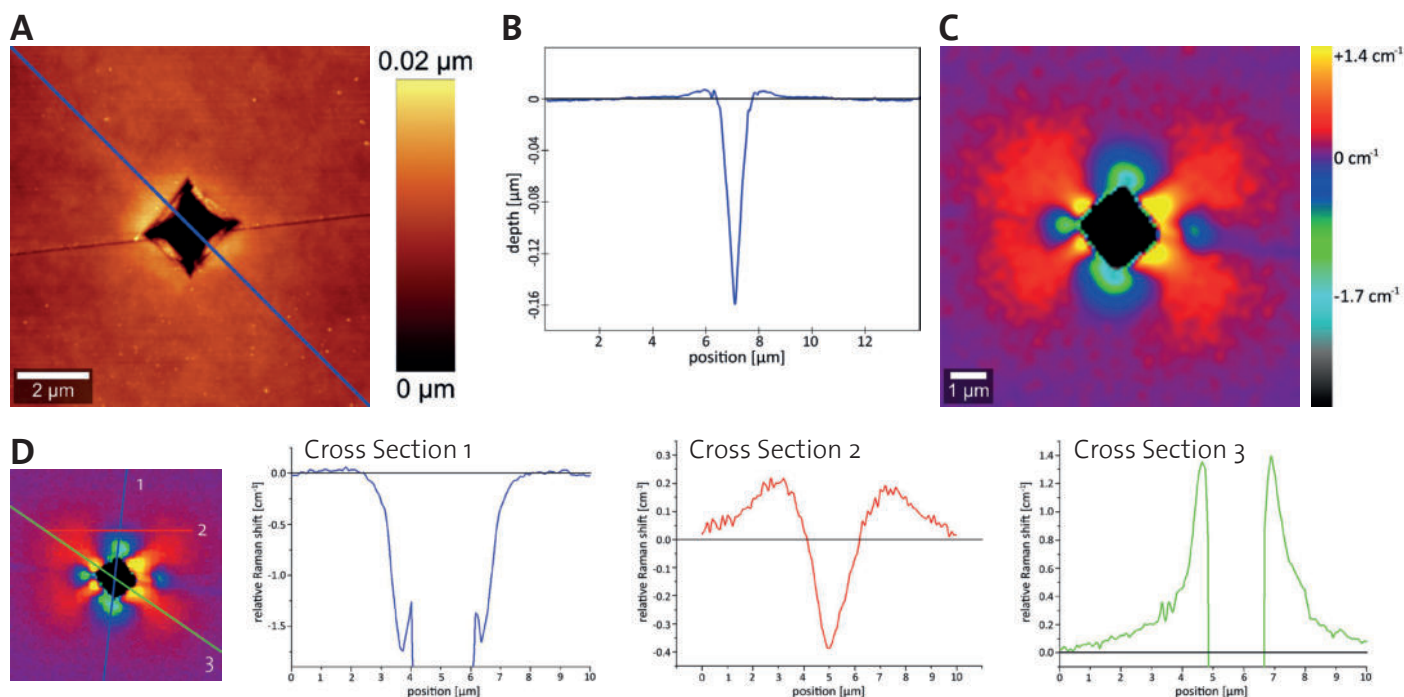


**Figure 5: Characterization of topography and stress in silicon around a Vickers indent.**

**A:** AFM image of the topography around an indent,  $10 \times 10\ \mu\text{m}^2$ .

**B:** Depth profile along the blue line in the AFM image (A).

**C:** Raman stress image of the same sample area as in A. The shift of the silicon Raman peak at  $520\text{ cm}^{-1}$  is color coded.

**D:** Stress profile cross sections along three different axes, named 1, 2 and 3.

Sample courtesy of Helmut Fischer GmbH, Sindelfingen, Germany.

## Correlative Raman-SEM imaging of strained nanopillars

Semiconducting nanostructures are investigated for their application in optoelectronic devices, for example, efficient solar cells. RISE (Raman Imaging and Scanning Electron) microscopy was applied here to study the physical properties of silicon nanopillars that were etched out of Si(111) and Si(100) substrates [6, 7]. A strain gradient, modifying the electronic band structure of the pillars, was introduced via wet thermal oxidation. High-resolution SEM images revealed the geometric dimensions of the nanopillars, with a height of 2 - 3  $\mu\text{m}$  and a diameter

of 500 nm or 700 nm, depending on the substrate. The symmetry of the nanopillars followed a densely-packed pattern (hexagonal symmetry) on both substrates (Figure 6).

Raman images were acquired from the same sample area by transferring the sample inside the vacuum chamber to the Raman measuring position [6]. From Raman spectra, it is possible to evaluate the crystallinity and stress state of the analyzed Si-sample [4, 5]. A shift of the silicon peak at  $520\text{ cm}^{-1}$  indicates stress in the sample, while low crystallinity leads to

a broadening of the band. Raman spectra acquired from the nanopillars are shown color coded in Figure 6. The Raman images of the two samples revealed different patterns of strain and crystallinity (Figure 6). On the (111) substrate, all pillars showed concentric regions of different strain levels (Figure 6A), while some pillars on the (100) substrate showed a more complex pattern (Figure 6B). The combination of Raman and SEM thus made it possible to correlate the high-resolution structural information of SEM with the Raman information on strain and crystallinity.

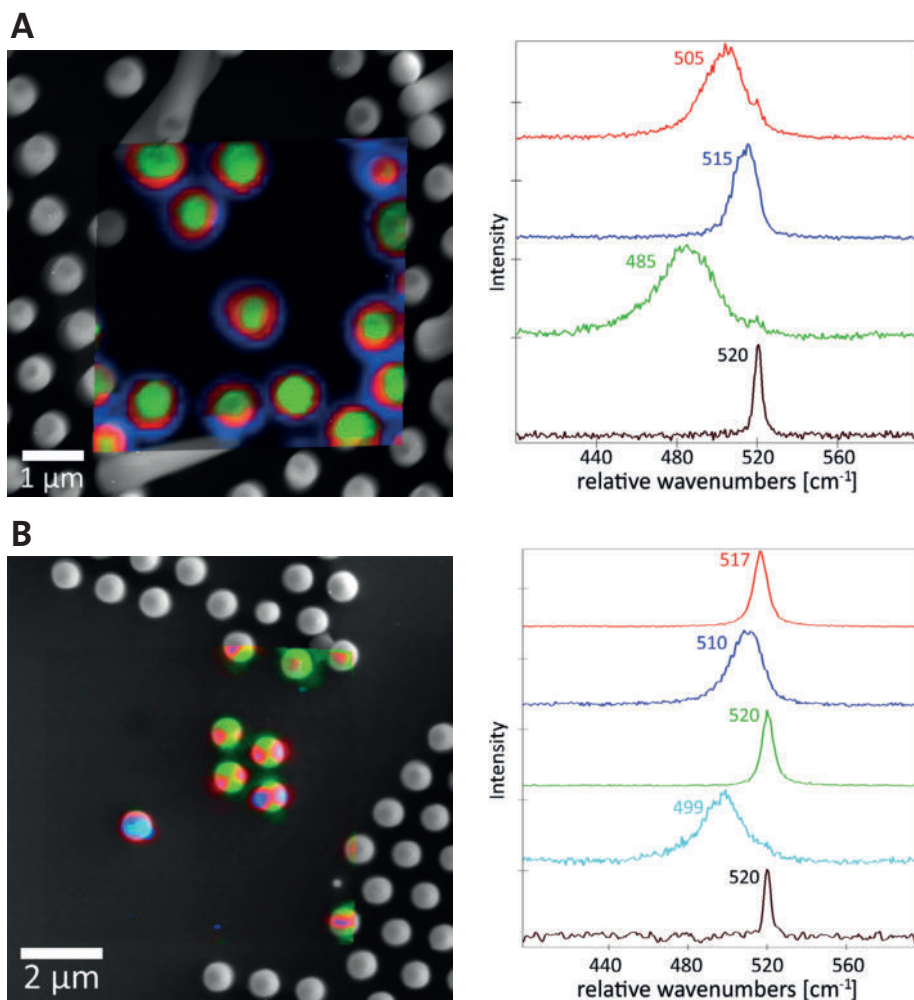


**Figure 6: RISE imaging of strained silicon pillars etched out of differently-oriented Si substrates.**

A section of the respective SEM image is overlaid with the Raman image of this region. The Raman image is color coded according to the spectra shown on the right. The respective maximum is indicated next to the peaks. Note the different scale bars and color codes in panels A and B.

**A:** Nanopillars etched out of a (111) silicon substrate.

**B:** Nanopillars etched out of a (100) silicon substrate.

Sample courtesy of Prof. Alois Lugstein (Institute for Solid State Electronics, Vienna University of Technology, Vienna, Austria).

## Correlative characterization of 2D semiconducting materials

Two-dimensional semiconducting materials, such as transition metal dichalcogenides (TMDs), are receiving increasing attention due to their unique physical, chemical and electronic properties. An important example is molybdenum disulfide ( $\text{MoS}_2$ ). Single-layer  $\text{MoS}_2$  is a direct band gap semiconductor, in contrast to bulk  $\text{MoS}_2$ , which has an indirect band gap. 2D  $\text{MoS}_2$  is thus investigated for its

potential applications in optoelectronic devices. As grain boundaries can affect the properties of 2D materials, sensitive and fast methods for their visualization are needed [8]. Here, we present correlative confocal Raman and nonlinear multi-photon imaging measurements that comprehensively characterize the crystal structure and local strain/doping effects at the crystal boundary of 2D materials.

The following experiments were performed using an alpha300 RA microscope equipped with a 488 nm laser for Raman measurements and a 1560 nm fs-pulsed laser for second and third harmonic generation (SHG and THG), at the Laboratory of Advanced Nanomaterials, Wuhan University, China. The sample was single-layer  $\text{MoS}_2$ , synthesized by chemical vapor deposition (CVD).

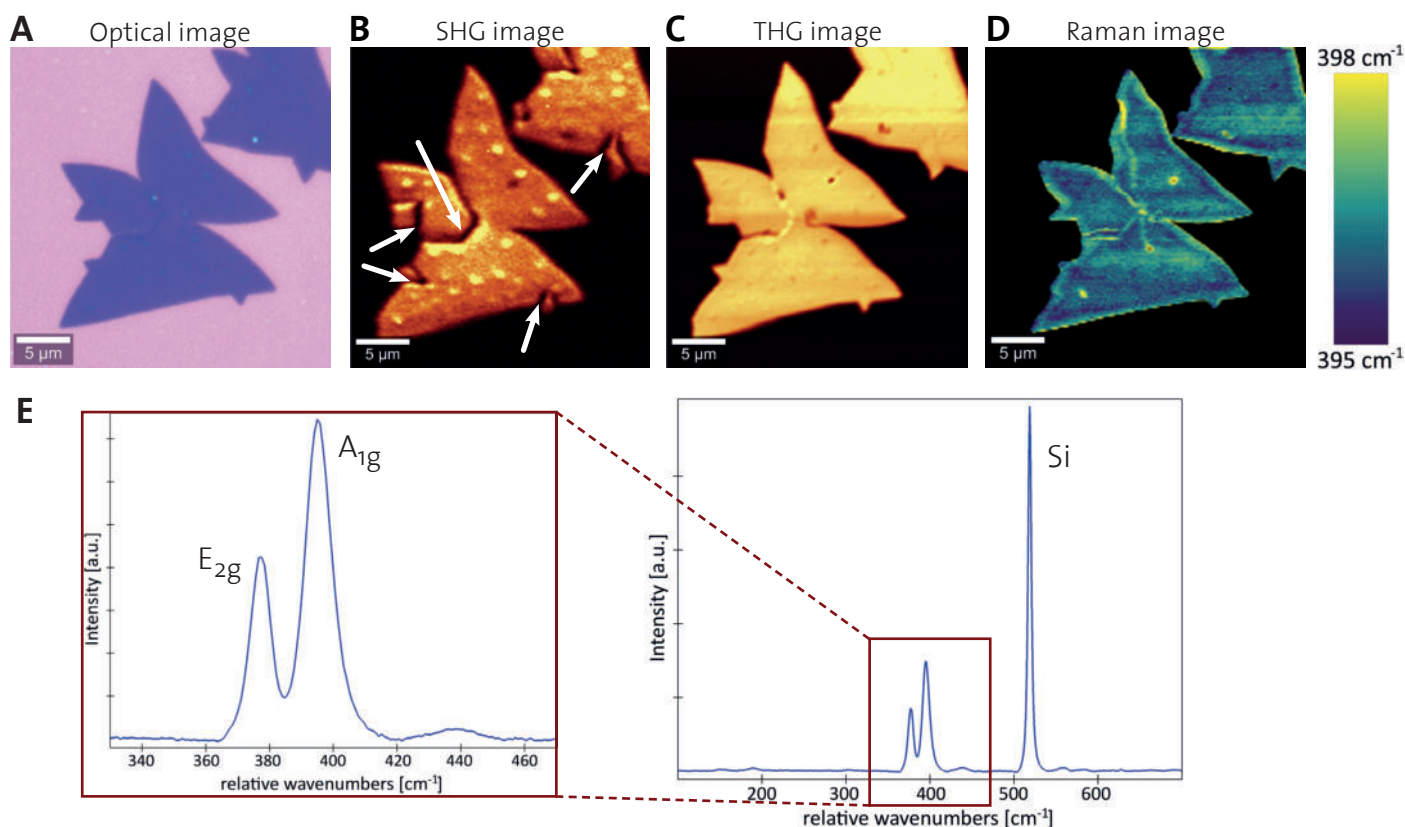


**Figure 7: Analysis of grain boundaries and strain on monolayer CVD  $\text{MoS}_2$ .**

**A:** Optical image.

**B:** SHG intensity image. Grain boundaries are indicated by white arrows.

**C:** THG intensity image.

**D:** Raman image displaying the position of the  $A_{1g}$  mode (see panel E).

**E:** Raman spectra averaged over the dark blue areas in panel D ( $A_{1g}$  peak positions between 395.0  $\text{cm}^{-1}$  and 395.5  $\text{cm}^{-1}$  relative wavenumbers). The peak at 520  $\text{cm}^{-1}$  originates from the silicon substrate.

Scan range for Raman, SHG, THG: 150 x 150 pixels in 30 x 30  $\mu\text{m}^2$ .

WITec is grateful to Prof. Lei Fu (Laboratory of Advanced Nanomaterials, Wuhan University, China) for granting access to his Raman microscope.



In the optical image, a crack in the crystal is faintly visible, but no other features can be discerned (Figure 7A). For more information, SHG and THG measurements were performed simultaneously (Figure 7B, C). SHG is a nonlinear optical process that radiates a photon with twice the frequency of the excitation photon. The SHG theory requires non-centric symmetry and is sensitive to changes in crystal symmetry, layer thickness, stacking order and crystal orientation [9]. SHG imaging is thus very useful for characterizing crystal structures of 2D materials. The SHG image revealed several grain boundaries in the MoS<sub>2</sub> flake (Figure 7B) that were not visible in the optical or THG images.

Further lattice features, such as the strain/doping change at the boundary, could

be revealed by high-resolution Raman imaging (Figure 7D, E). The exact positions of the in-plane E<sub>2g</sub> and out-of-plane A<sub>1g</sub> peaks (Figure 7E) were quantified for every image pixel by fitting a double Lorentzian function. In the resulting Raman image, the frequency of the A<sub>1g</sub> mode was color coded (Figure 7D). In all recorded Raman spectra, both the E<sub>2g</sub> and A<sub>1g</sub> Raman modes were obviously red-shifted compared to published data on monolayer MoS<sub>2</sub> [8, 10]. A calibration artifact can be ruled out because the Rayleigh peak and the silicon Raman peak were at 0 cm<sup>-1</sup> and 520 cm<sup>-1</sup> relative wavenumbers, respectively, as expected. The red-shift of the E<sub>2g</sub> and A<sub>1g</sub> peaks implies that the investigated flake was under strong tensile strain over its entire area. However, the high-resolution

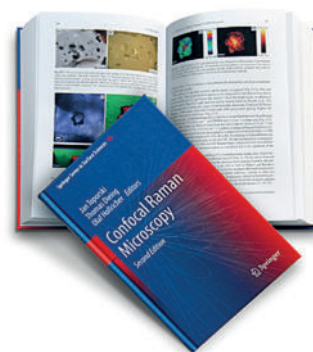
Raman image revealed local differences, such as areas with reduced strain (yellow in Figure 7D). A similar study recently used multi-photon, Raman and photoluminescence microscopy for visualizing grain boundaries in monolayer MoS<sub>2</sub> [8]. Correlative SHG and Raman imaging could not only make the boundaries visible but also demonstrate the strain change, providing a comprehensive understanding of crystal symmetry and lattice. These examples illustrate the utility of correlative non-linear imaging (SHG/THG) and Raman imaging for characterizing 2D materials and optoelectronic, ferroelectric or ferromagnetic devices. Changes of structure and strain at the grain boundaries could easily be visualized at the same sample location.

## References

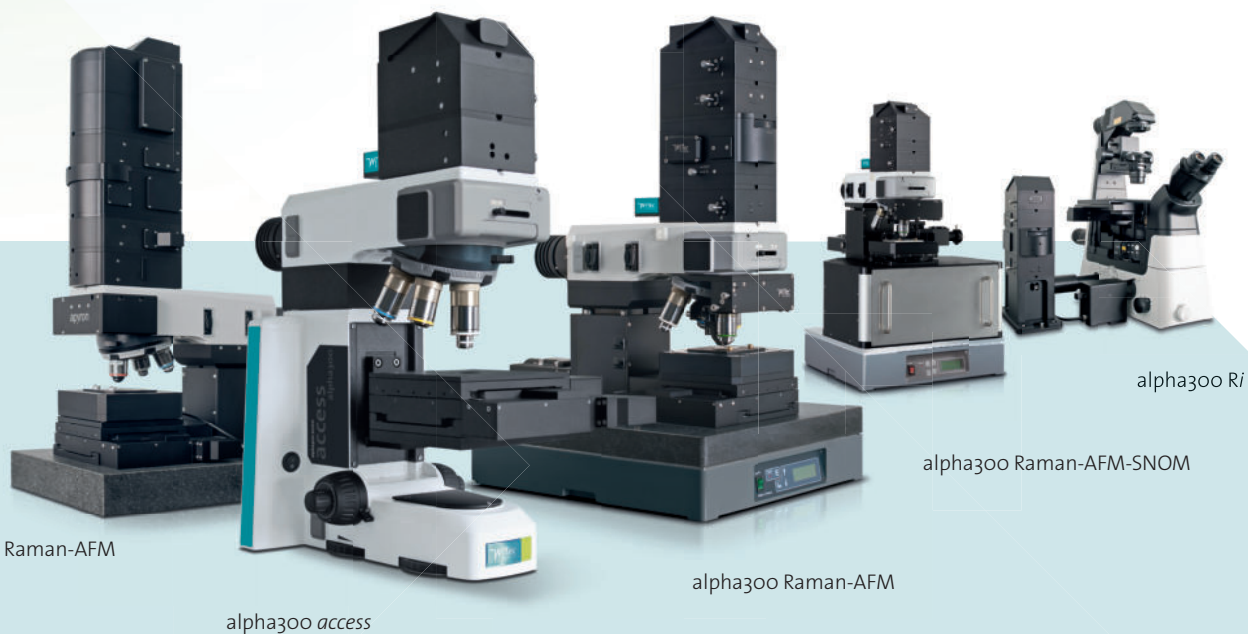
- [1] B. Kann, M. Windbergs, *Chemical imaging of drug delivery systems with structured surfaces – a combined analytical approach of confocal Raman microscopy and optical profilometry*. The AAPS Journal, 2013, **15**: p. 505-510. DOI: 10.1208/s12248-013-9457-7.
- [2] M. Kuball, *Raman spectroscopy of GaN, AlGaN and AlN for process and growth monitoring/control*. Surface and Interface Analysis, 2001, **31**: p. 987-999. DOI: 10.1002/sia.1134.
- [3] J.T. Holmi, B.H. Bairamov, S. Suihkonen, H. Lipsanen, *Identifying threading dislocation types in ammonothermally grown bulk  $\alpha$ -GaN by confocal Raman 3-D imaging of volumetric stress distribution*. Journal of Crystal Growth, 2018, **499**: p. 47-54. DOI: 10.1016/j.jcrysgro.2018.07.024.
- [4] U. Schmidt, W. Ibach, J. Müller, K. Weishaupt, O. Hollricher, *Raman spectral imaging — A nondestructive, high resolution analysis technique for local stress measurements in silicon*. Vibrational Spectroscopy, 2006, **42**: p. 93-97. DOI: 10.1016/j.vibspec.2006.01.005.
- [5] I. De Wolf, *Micro-Raman spectroscopy to study local mechanical stress in silicon integrated circuits*. Semiconductor Science and Technology, 1996, **11**: p. 139-154. DOI: 10.1088/0268-1242/11/2/001.
- [6] J. Jiruše, M. Haničinec, M. Havelka, O. Hollricher, W. Ibach, P. Spizig, *Integrating focused ion beam-scanning electron microscope with confocal Raman microscope into a single instrument*. Journal of Vacuum Science & Technology B, 2014, **32**: o6FC03. DOI: 10.1116/1.4897502.
- [7] U. Schmidt, K. Hollricher, P. Ayasse, O. Hollricher, *Correlative RISE microscopy: Raman imaging meets scanning electron probe microscopy*. Microscopy and Analysis, 2015, **29**: p. 24-27.
- [8] L. Karvonen, A. Säynätjoki, M.J. Huttunen, A. Autere, B. Amirsolaimani, S. Li, R.A. Norwood, N. Peyghambarian, H. Lipsanen, G. Eda, K. Kieu, Z. Sun, *Rapid visualization of grain boundaries in monolayer MoS<sub>2</sub> by multiphoton microscopy*. Nature Communications, 2017, **8**: 15714. DOI: 10.1038/ncomms15714.
- [9] X. Yin, Z. Ye, D.A. Chenet, Y. Ye, K. O'Brien, J.C. Hone, X. Zhang, *Edge nonlinear optics on a MoS<sub>2</sub> atomic monolayer*. Science, 2014, **344**: p. 488-490. DOI: 10.1126/science.1250564.
- [10] H. Li, Q. Zhang, C.C.R. Yap, B.K. Tay, T.H.T. Edwin, A. Olivier, D. Baillargeat, *From Bulk to Monolayer MoS<sub>2</sub>: Evolution of Raman Scattering*. Advanced Functional Materials, 2012, **22**: p. 1385-1390. DOI: 10.1002/adfm.201102111.
- [11] J. Toporski, T. Dieing, O. Hollricher, eds. *Confocal Raman Microscopy*. 2<sup>nd</sup> ed. 2018, Springer International Publishing AG. DOI: 10.1007/978-3-319-75380-5.

For more information on confocal Raman imaging and its applications, see the book:

**Confocal Raman Microscopy** [11]



## WITec Microscopes



apyron  
automated Raman-AFM

alpha300 access

alpha300 Raman-AFM

alpha300 Raman-AFM-SNOM

alpha300 Ri

### WITec Headquarters

WITec GmbH  
Lise-Meitner-Str. 6  
D-89081 Ulm . Germany  
Phone +49 (0) 731 140700  
Fax +49 (0) 731 14070200  
info@WITec.de  
www.WITec.de

### WITec North America

WITec Instruments Corp.  
130G Market Place Blvd.  
Knoxville . TN 37922 . USA  
Phone 865 984 4445  
Fax 865 984 4441  
info@WITec-Instruments.com  
www.WITec-Instruments.com

### WITec South East Asia

WITec Pte. Ltd.  
25 International Business Park  
#03-59A German Centre  
Singapore 609916  
Phone +65 9026 5667  
shawn.lee@WITec.biz  
www.WITec.de

### WITec China

WITec Beijing Representative Office  
Unit 507, Landmark Tower 1  
8 North Dongsanhuan Road  
Beijing, PRC., 100004  
Phone +86 (0) 10 6590 0577  
info.China@WITec-Instruments.com  
www.WITec.de/cn

### WITec Japan

WITec K. K.  
1-1-5 Furo-cho, Naka-ku,  
Yokohama City, Kanagawa Pref.  
231-0032 Japan  
info@WITec.jp  
www.WITec.de/jp